

Supplementary Information

A smart organic gel template as metal cation and inorganic anions sensor

Novina Malviya,^a Mriganka Das,^a Poulami Mandal,^a and Suman Mukhopadhyay^{*a,b}

^a*Department of Chemistry, School of Basic Sciences, Indian Institute of Technology Indore, Simrol 453552 Indore, India.*

^b*Center for Bioscience and Biomedical Engineering, Indian Institute of Technology Indore, Simrol 453552 Indore, India.*

Email: suman@iiti.ac.in

Table of Contents

- Fig. S1.** FT-IR spectrum of gelator (**G1**).
- Fig. S2.** ^1H NMR spectrum of gelator (**G1**).
- Fig. S3.** ^{13}C NMR spectrum of gelator (**G1**).
- Fig. S4.** ESI- Mass spectrum of gelator (**G1**).
- Fig. S5.** "Inversion of a test tube" method
- Fig. S6.** FT-IR spectra of xerogel of **G1**.
- Fig. S7.** Partial ^1H NMR spectra of **G1** in DMSO d_6 at different concentrations:(a) 20 mM; (b) 100 mM; (c) 150 mM.
- Fig. S8.** Photographs of Sol-Gel of gelator **G1** in DMF and **G1** in the presence of various metal ions (using their perchlorate salts as the sources, **G1**: cation =2:1) under day light.
- Fig. S9-S13.** FT-IR spectra of xerogel of **ZnG1**, **NiG1**, **CuG1**, **Fe^{II}G1**, **Fe^{III}G1**.
- Fig. S14-S17.** FT-IR spectra of xerogel of **ZnG1+Br⁻**,**NiG1+CN⁻**, **CuG1+SCN⁻**, **Fe^{II}G1+S²⁻**.
- Fig. S18.** Fluorescence spectra of (a) **ZnG1** (b) **NiG1** (c) **CuG1** (d) **FeG1** in the presence of mixture of anions at room temperature.
- Fig. S19.** (a) Fluorescence spectra of **ZnG1** with increasing concentration of **Br⁻** (using 0.01M **KBr** water solution as the **Br⁻** sources); (b) Fluorescence spectra of **NiG1** with increasing concentration of **CN⁻** (using 0.01M **NaCN** water solution as the **CN⁻** sources),(c) Fluorescence spectra of **CuG1** with increasing concentration of **SCN⁻** (using 0.01M **NaSCN** water solution as the **SCN⁻** sources); (d) Fluorescence spectra of **FeG1** with increasing concentration of **S²⁻**(using 0.01M **Na₂S** water solution as the **S²⁻** sources), $\lambda_{\text{ex}} = 350$ nm.
- Fig. S20-S23.** Linear viscoelastic (LSV) and Frequency sweep (FS) rheometry of **ZnG1**, **CuG1**, **NiG1**, **FeG1** The angular frequency (rad/s), storage modulus **G'** (Pa) and loss modulus **G''** (Pa) are shown as log scale.
- Fig. S24-S27.** SEM images of xerogel of **ZnG1**, **NiG1**, **FeG1**, **CuG1**.
- Fig. S28.** Powder XRD patterns of xerogel of **ZnG1**, **CuG1**, **NiG1**, **FeG1**.
- Fig. S29.** Powder XRD patterns of xerogel of **ZnG1+Br⁻**, **CuG1+SCN⁻**, **NiG1+CN⁻**, **FeG1+S²⁻**.

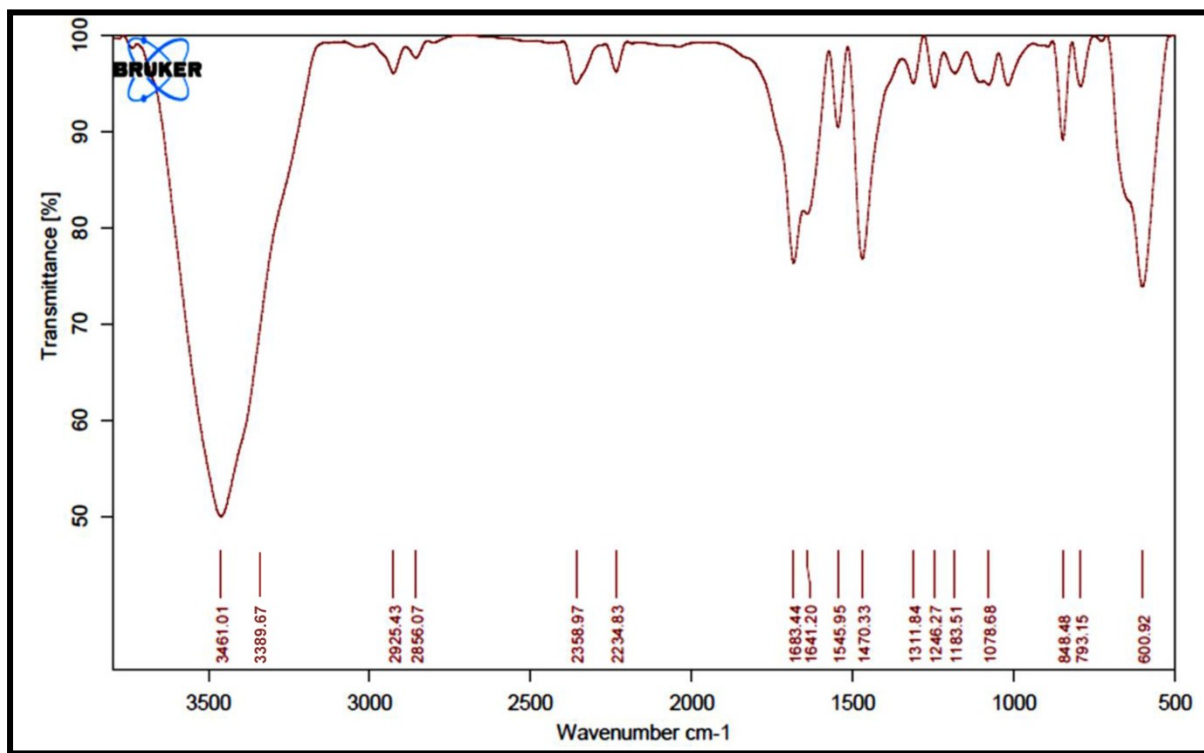


Fig. S1 FT-IR spectrum of gelator molecule **G1**.

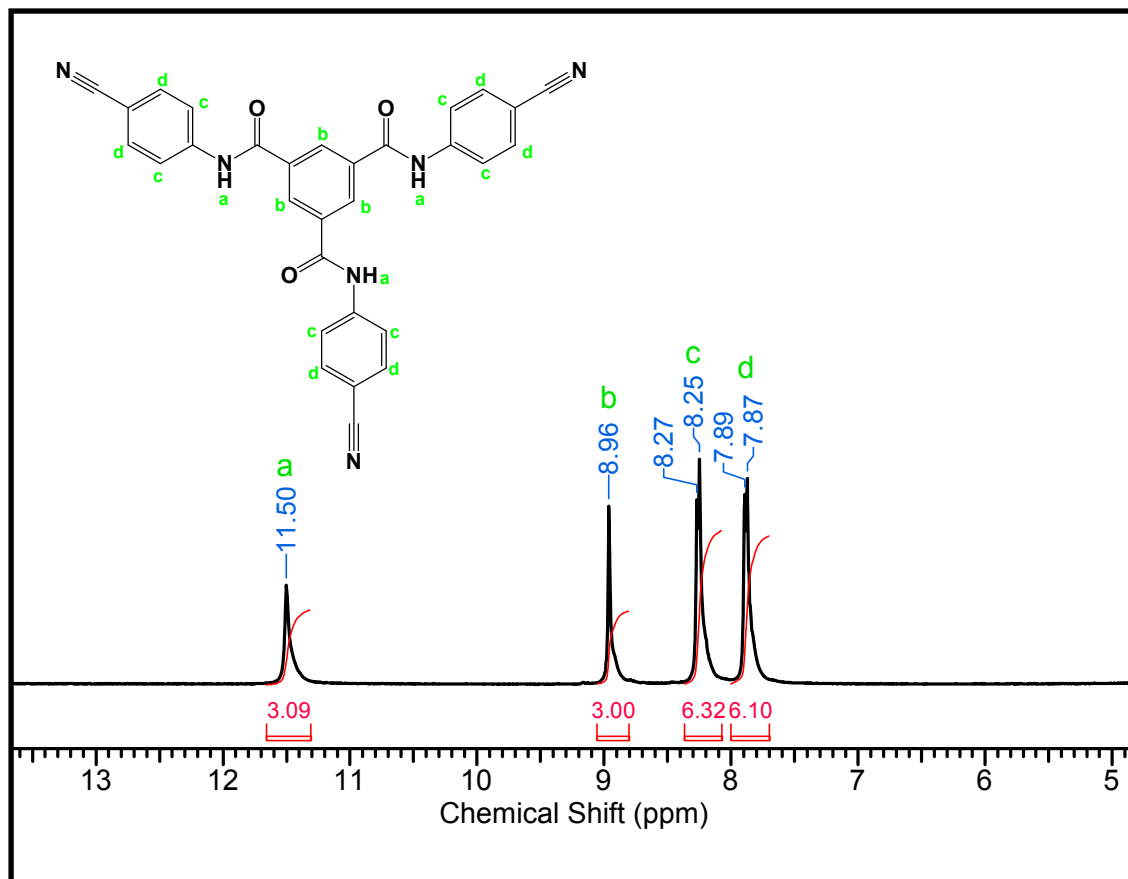


Fig. S2 ^1H NMR spectrum of gelator molecule **G1**.

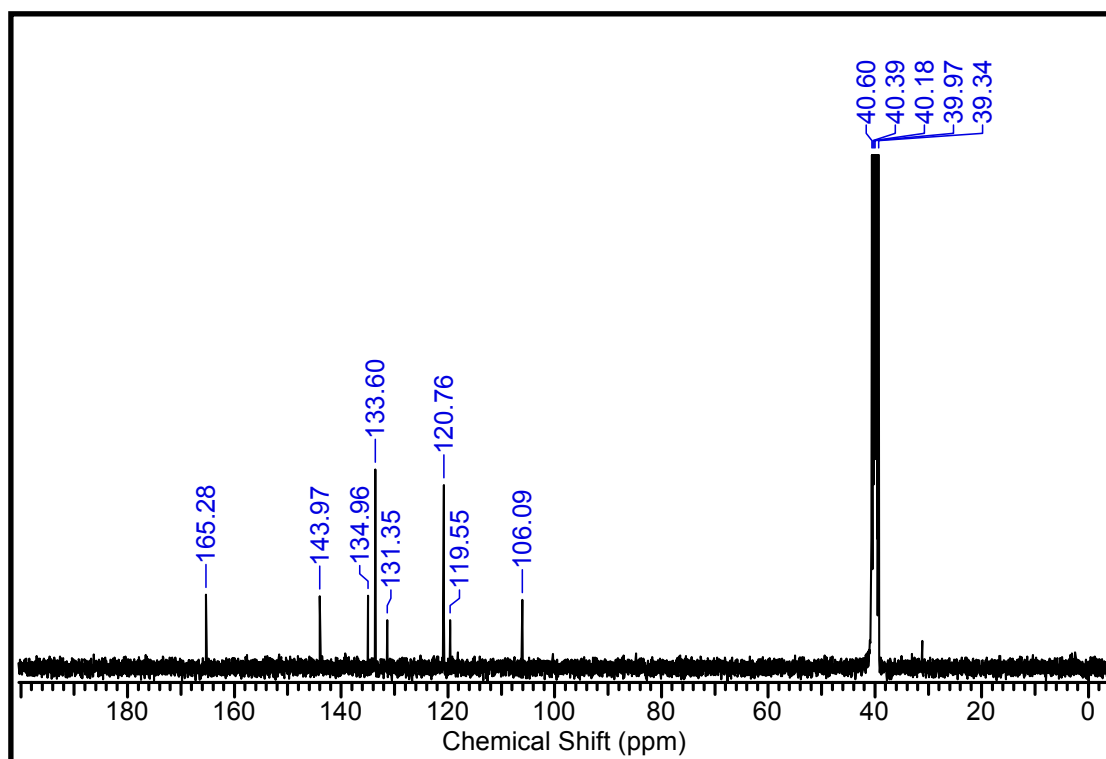


Fig. S3 ^{13}C NMR spectrum of gelator molecule **G1**.

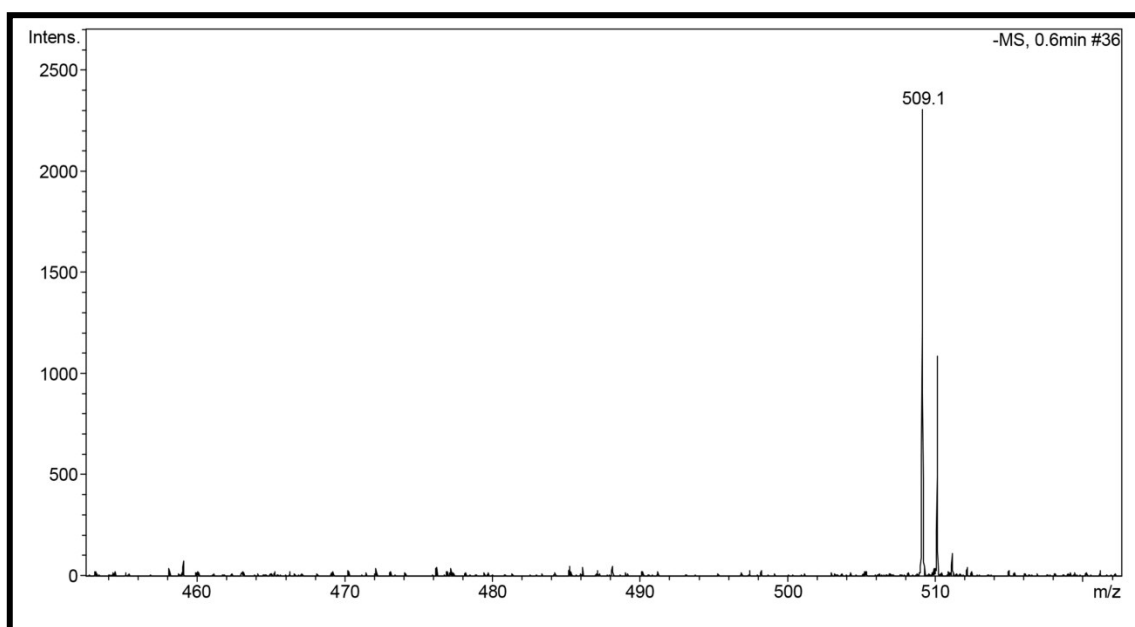


Fig. S4 ESI- Mass spectrum of gelator molecule **G1**.

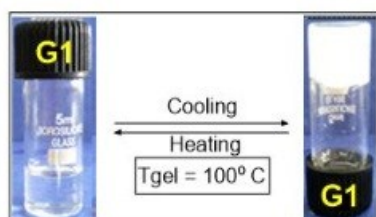


Fig. S5 "Inversion of a test tube" method.

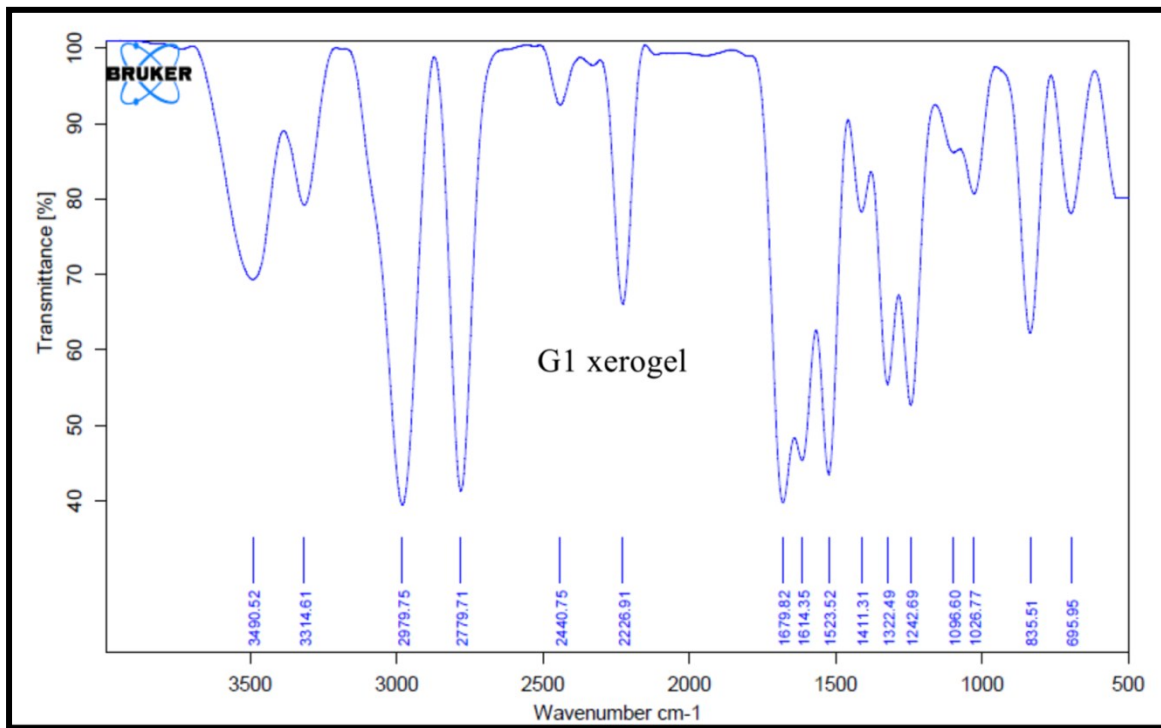


Fig. S6 FT-IR spectra of xerogel of **G1**.

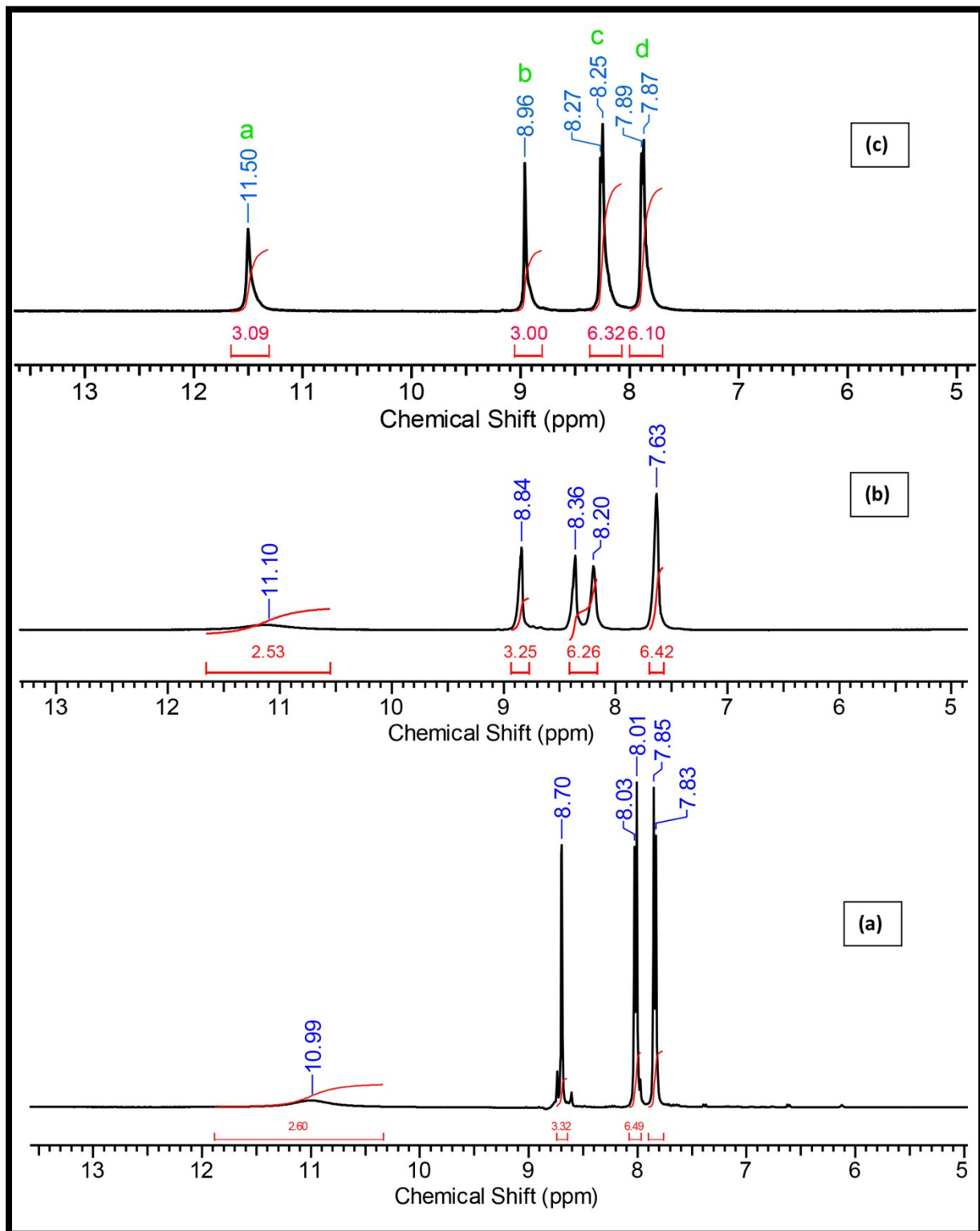


Fig. S7 Partial ^1H NMR spectra of G1 in DMSO-d_6 at different concentrations:(a) 20 mM (b) 100 mM (c) 150 mM.

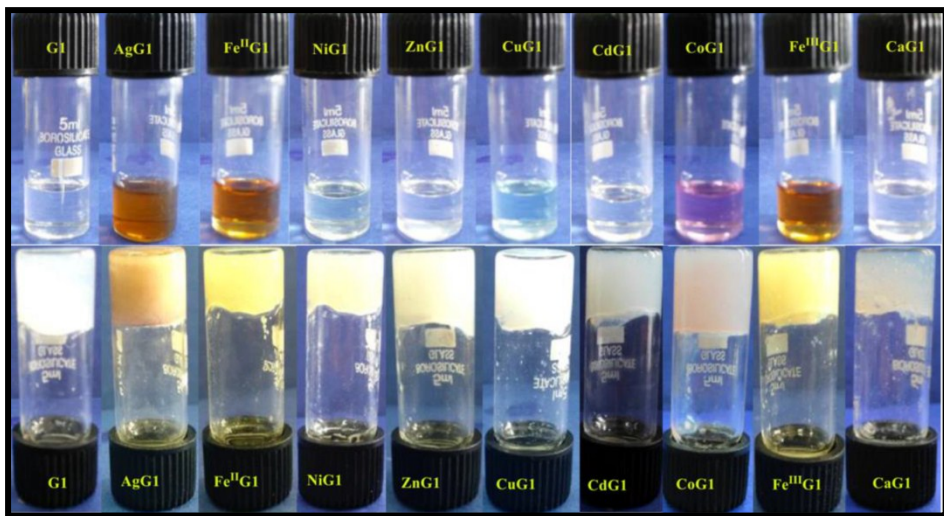
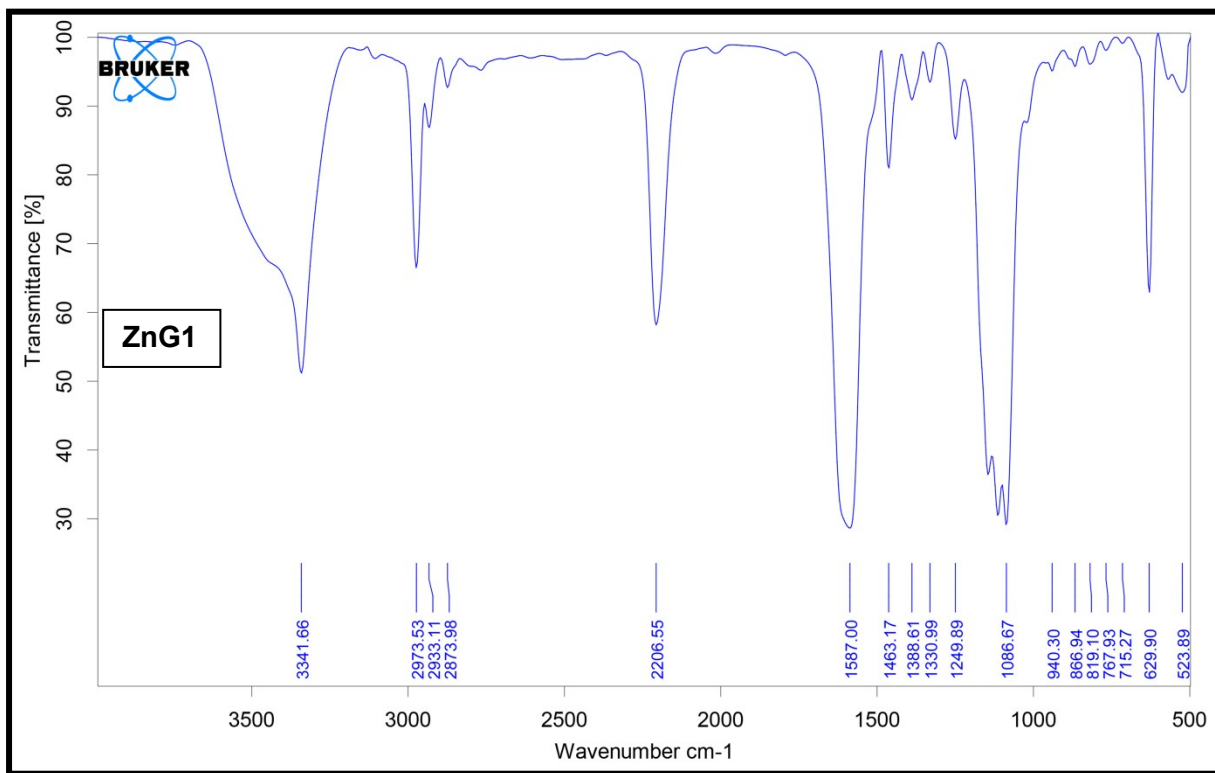
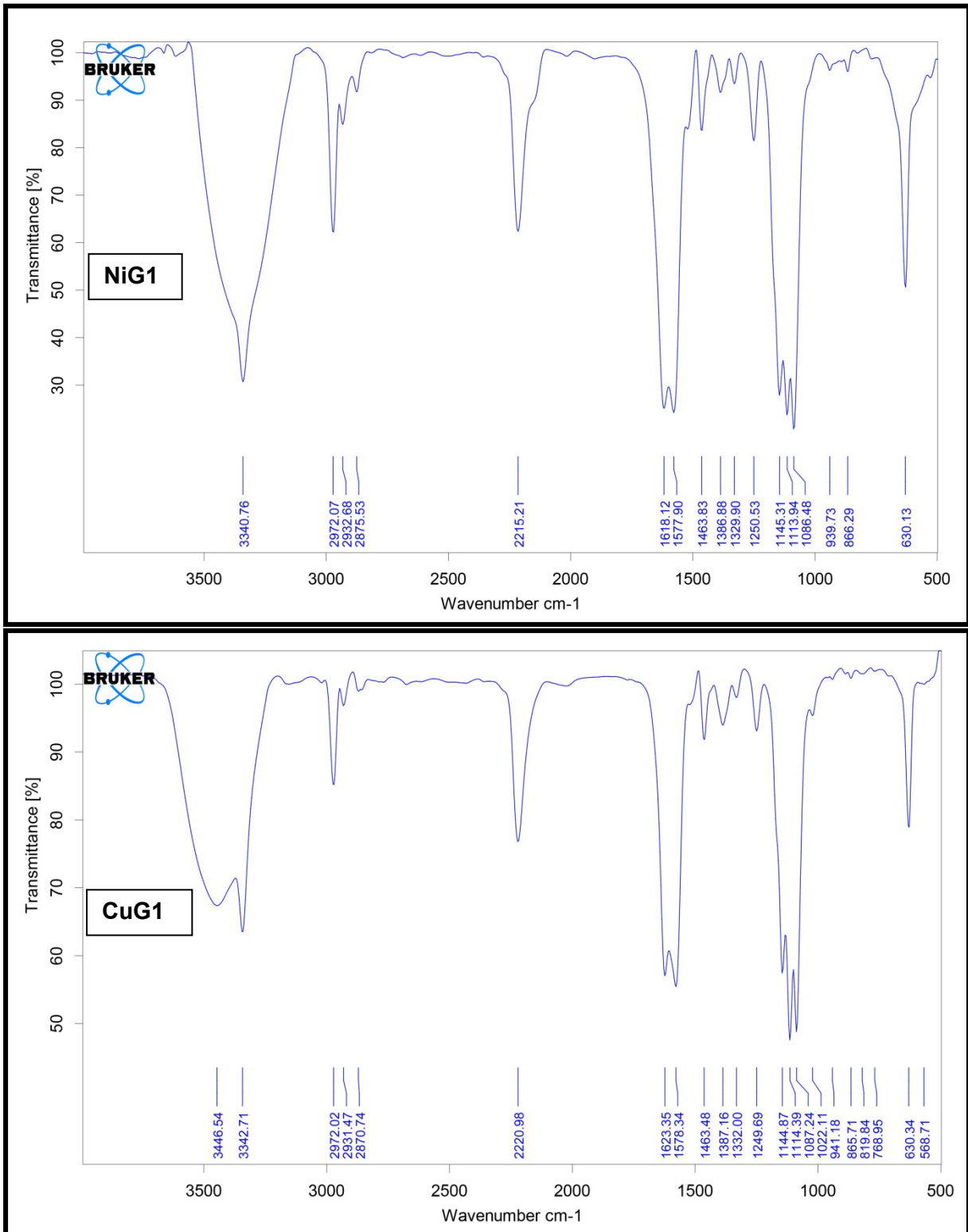


Fig. S8 Photographs of Sol-Gel of gelator **G1** in DMF and **G1** in the presence of various metal ions (using their perchlorate salts as the sources, **G1** : cation = 2:1) under day light.





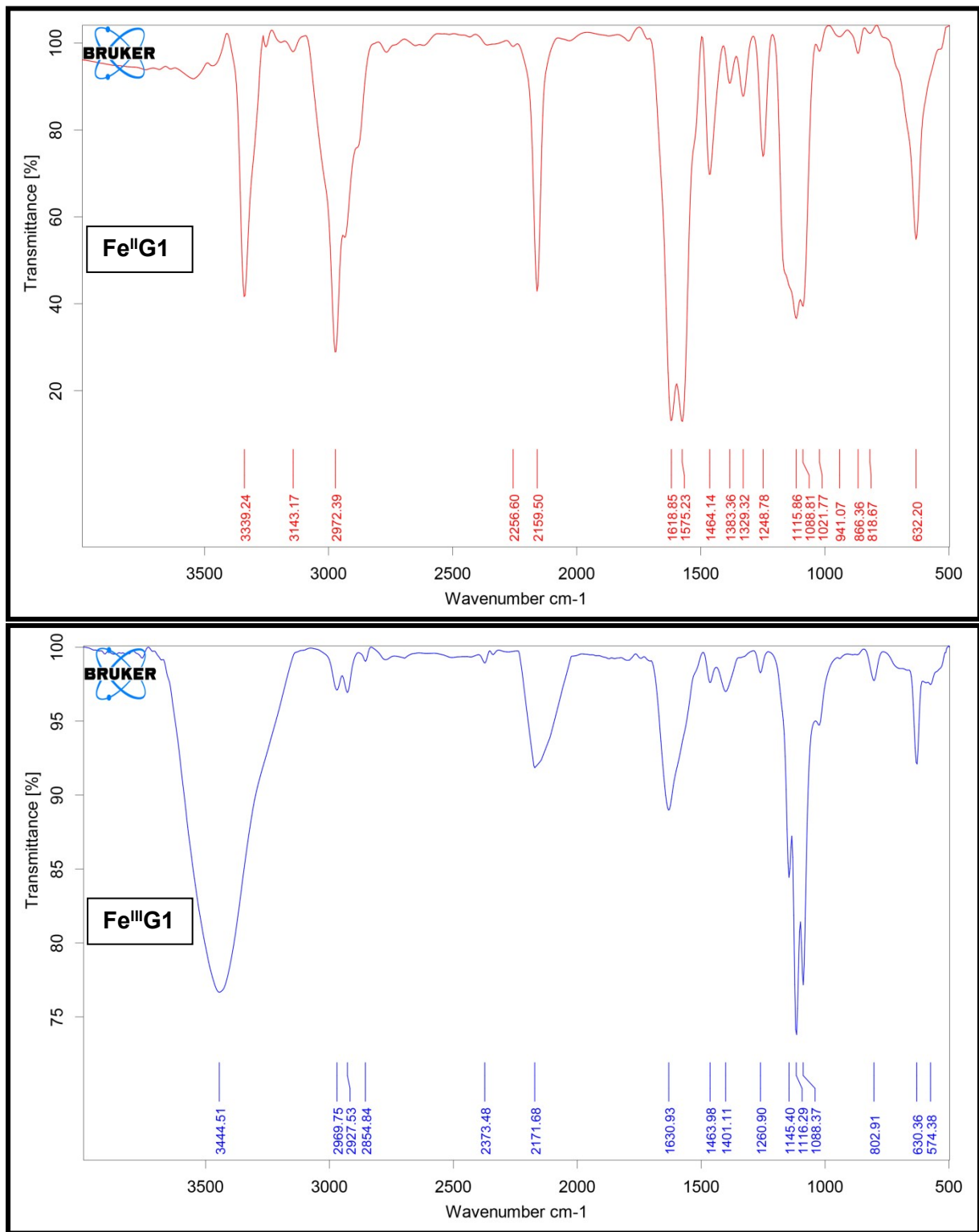
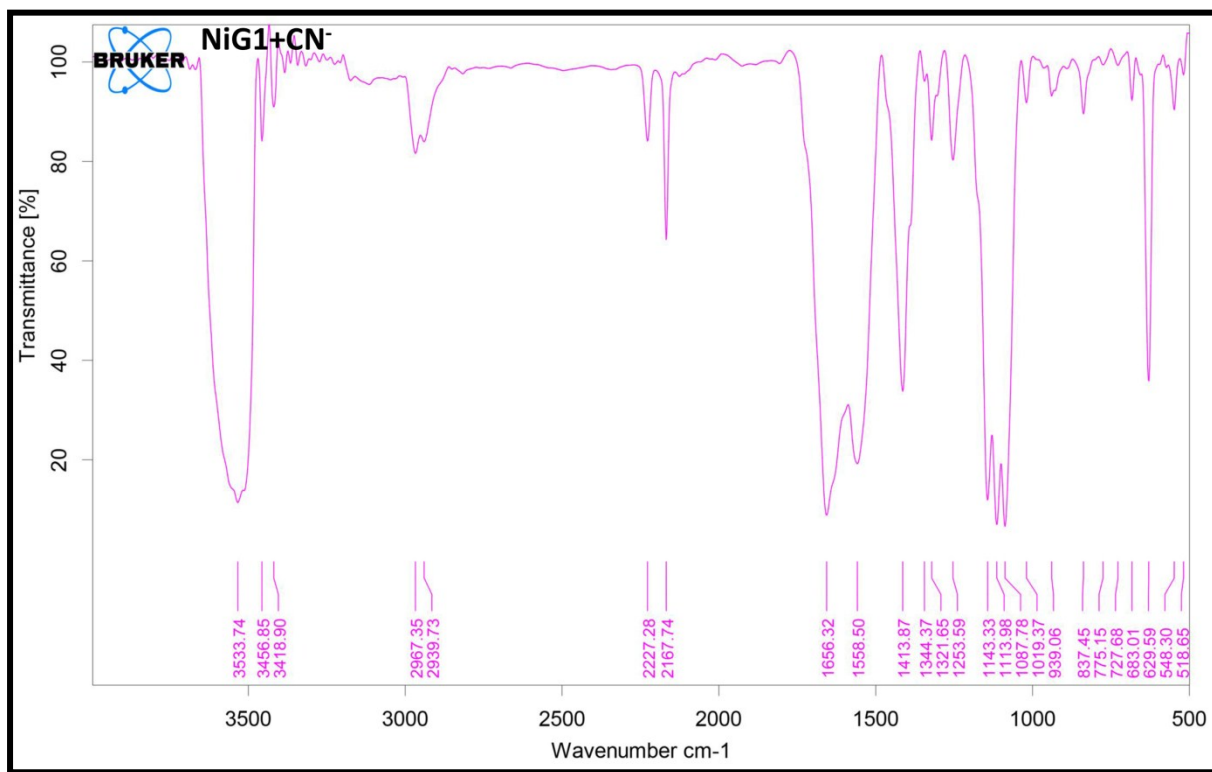
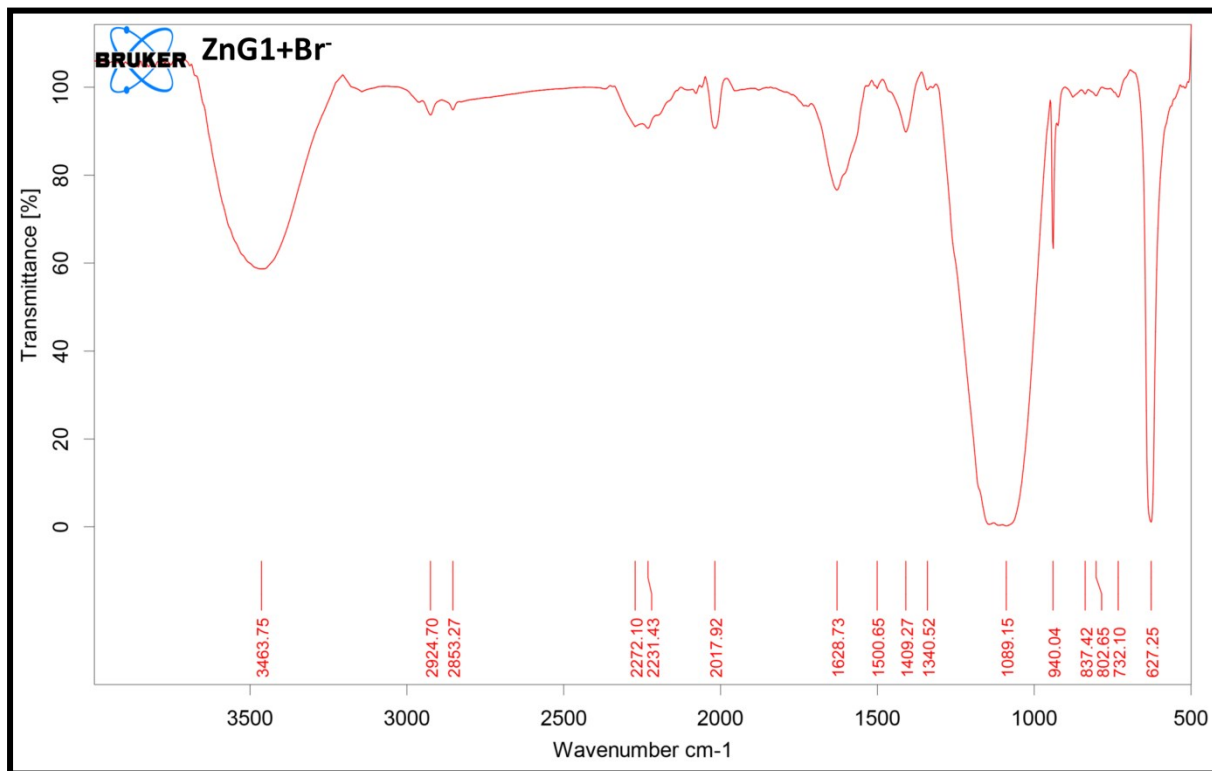


Fig. S9-S13 FT-IR spectra of xerogel of **ZnG1**, **NiG1**, **CuG1**, **Fe^{II}G1**, **Fe^{III}G1**.



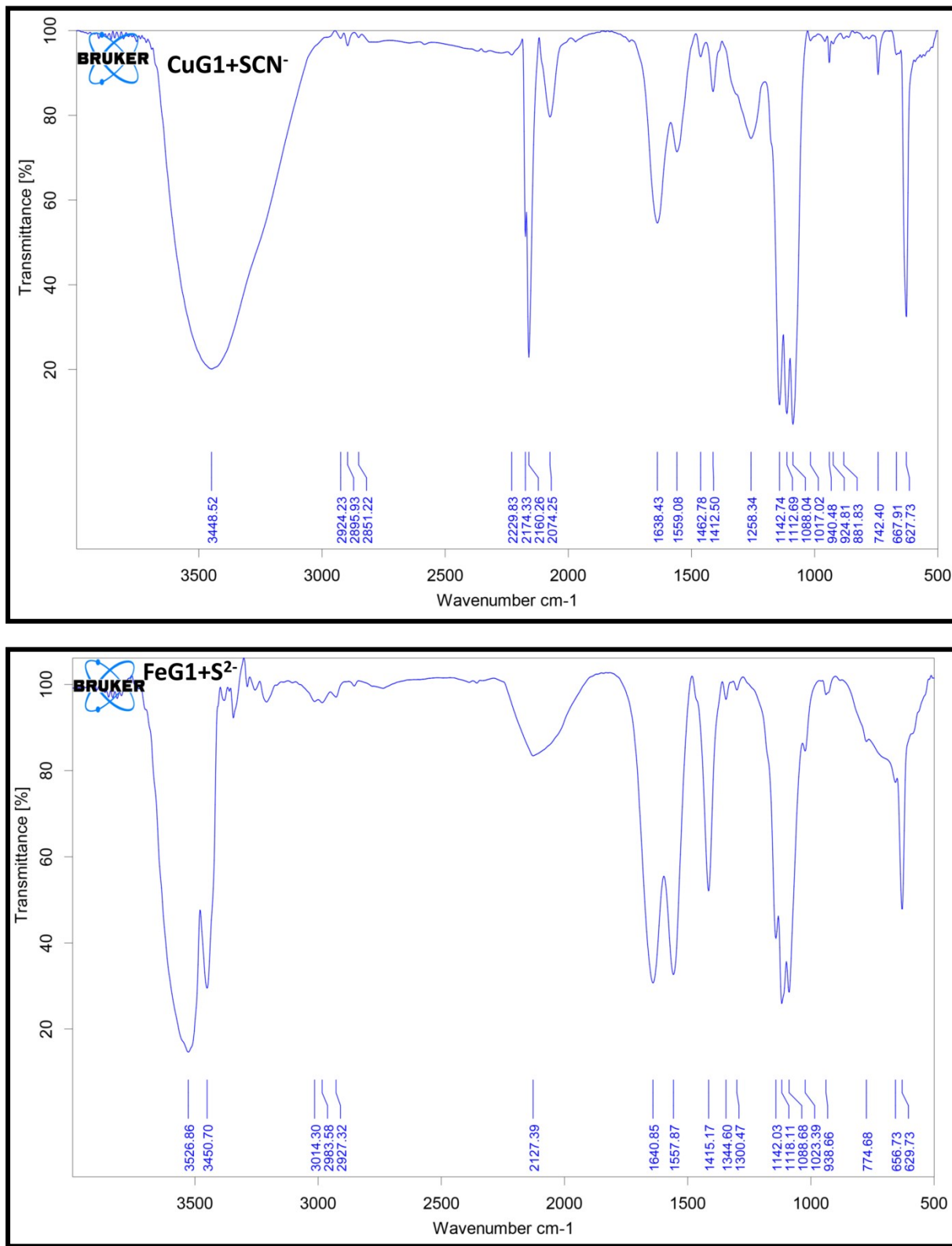


Fig. S14-S17. FT-IR spectra of xerogel of ZnG1+Br⁻, NiG1+CN⁻, CuG1+SCN⁻, Fe^{II}G1+S²⁻.

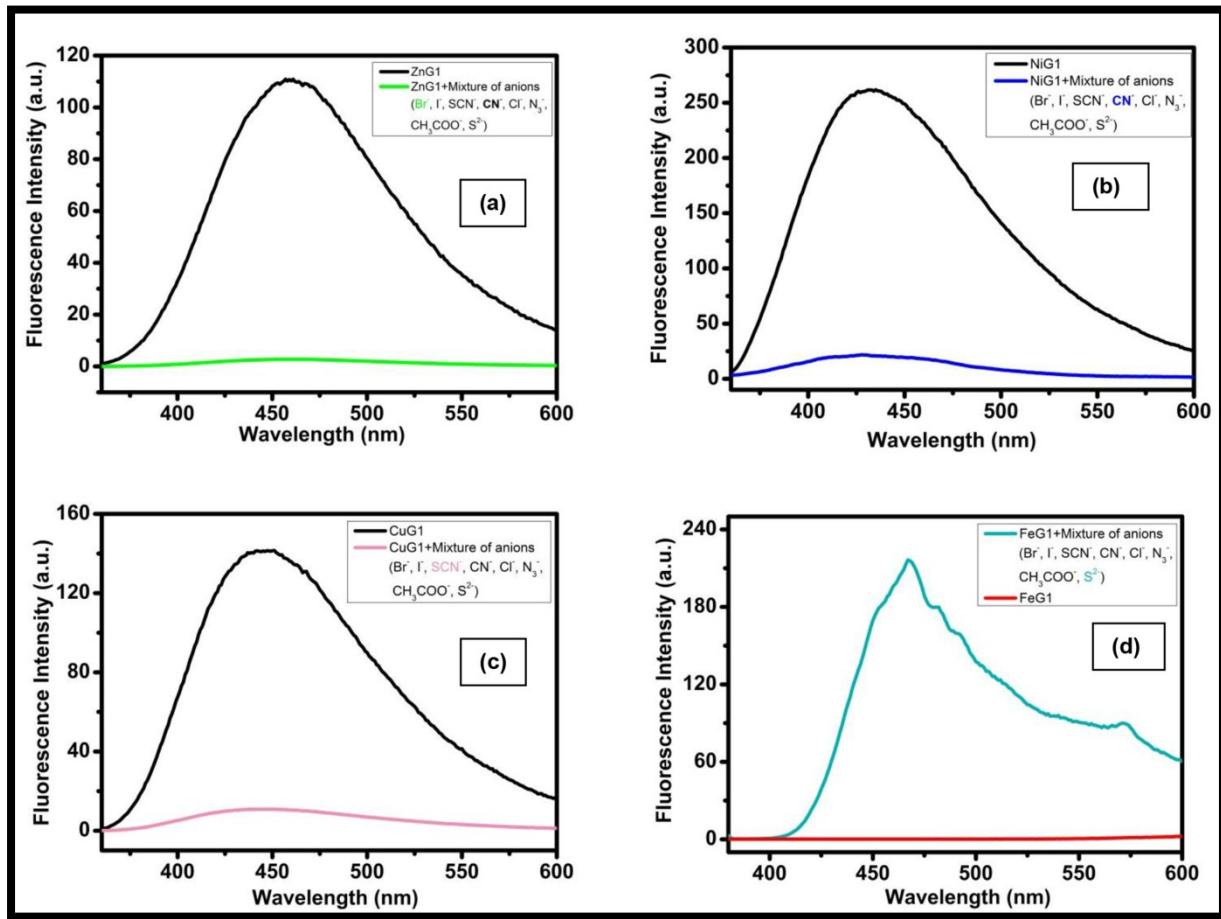
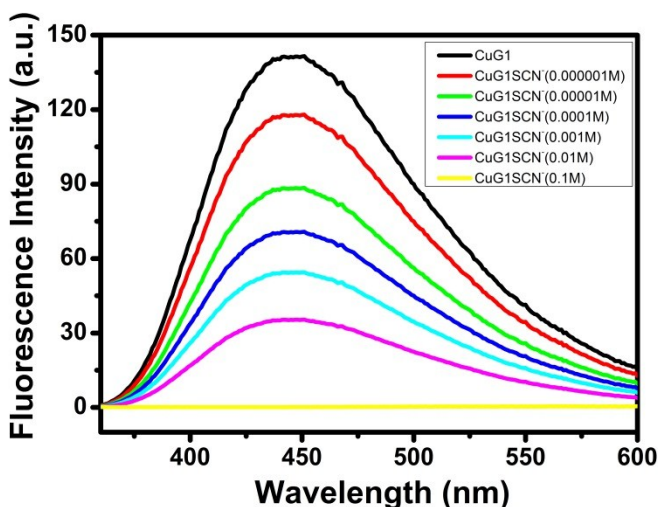
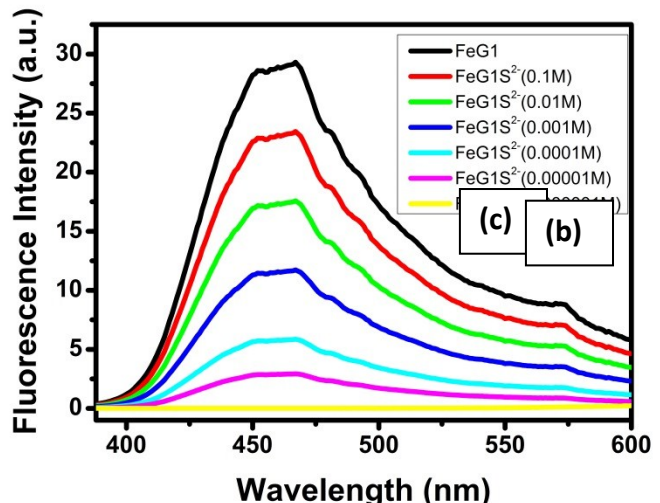
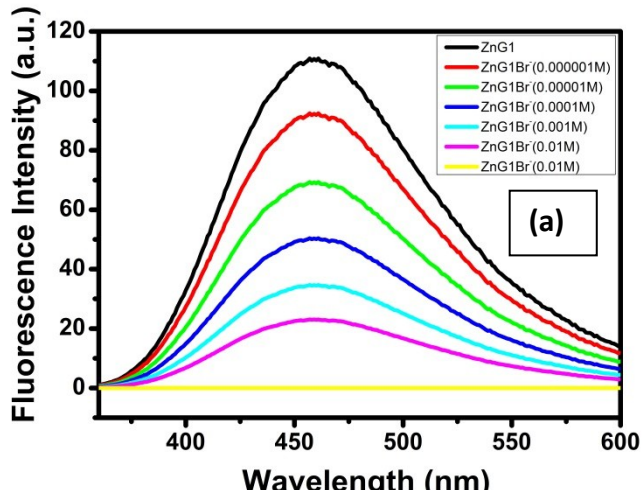


Fig. S18 Fluorescence spectra of (a) **ZnG1** (b) **NiG1** (c) **CuG1** (d) **FeG1** in the presence of mixture of anions at room temperature.



0.01M **NaSCN** water solution as the SCN^- sources); (d) Fluorescence spectra of **FeG1** with increasing concentration of S^{2-} (using 0.01M **Na₂S** water solution as the S^{2-} sources), $\lambda_{\text{ex}} = 350 \text{ nm}$.

Fig. S19 (a) Fluorescence spectra of **ZnG1** with increasing concentration of Br^- (using 0.01M **KBr** water solution as the Br^- sources); (b) Fluorescence spectra of **NiG1** with increasing concentration of CN^- (using 0.01M **NaCN** water solution as the CN^- sources),(c) Fluorescence spectra of **CuG1** with increasing concentration of SCN^- (using

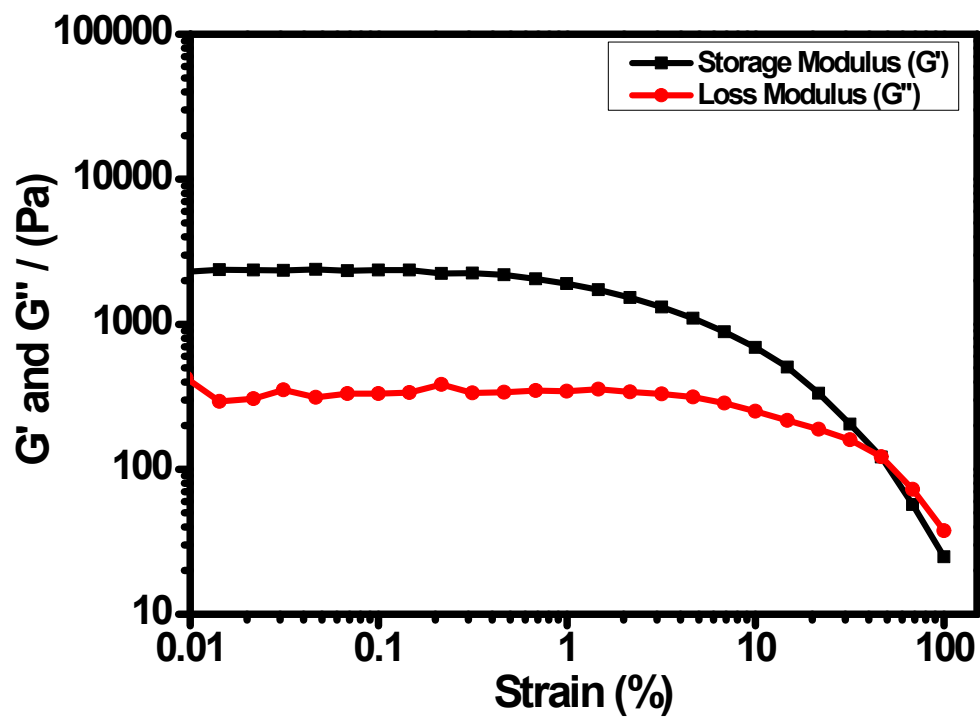


Fig. S20(a) Linear viscoelastic (LVE) property of **FeG1**.

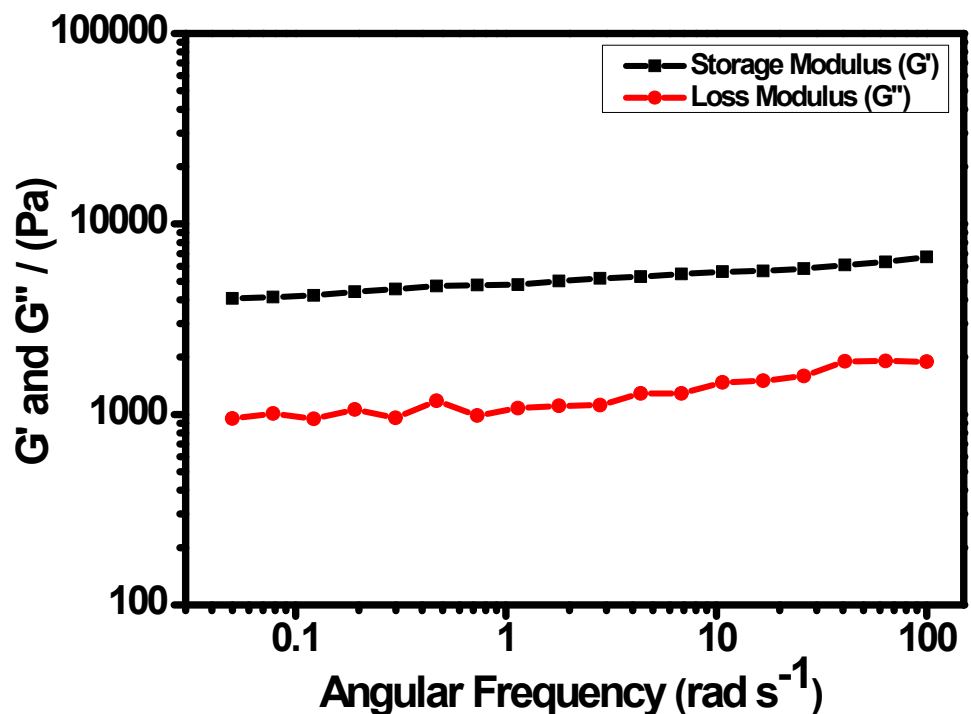


Fig. S20(b) The dynamic frequency sweep rheometry of **FeG1**. (Storage modulus G' is higher than the loss modulus G'').

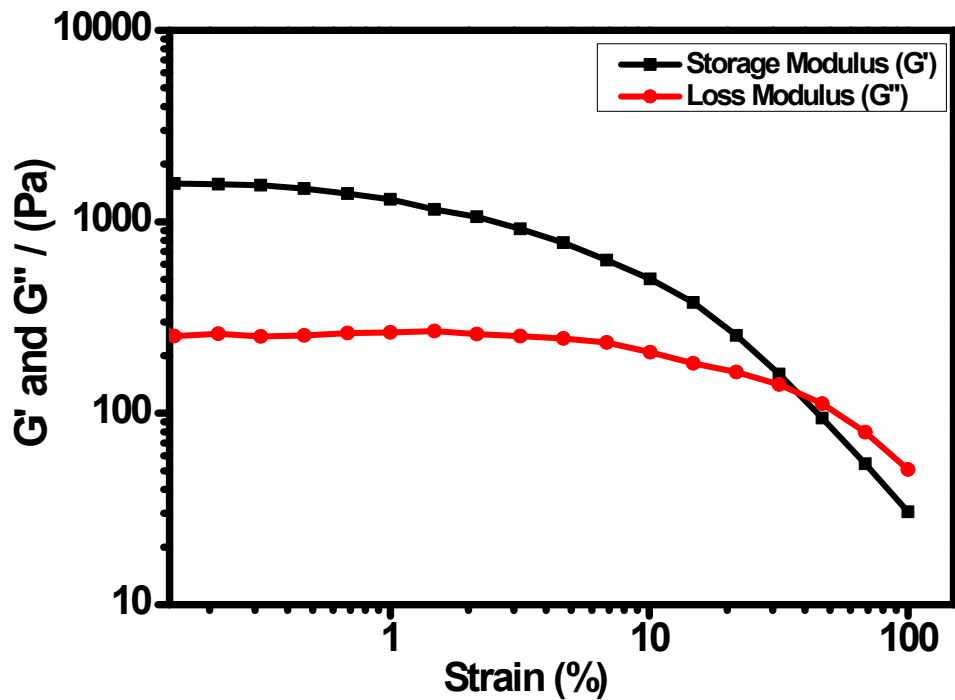


Fig. S21(a) Linear viscoelastic (LVE) property of CuG1.

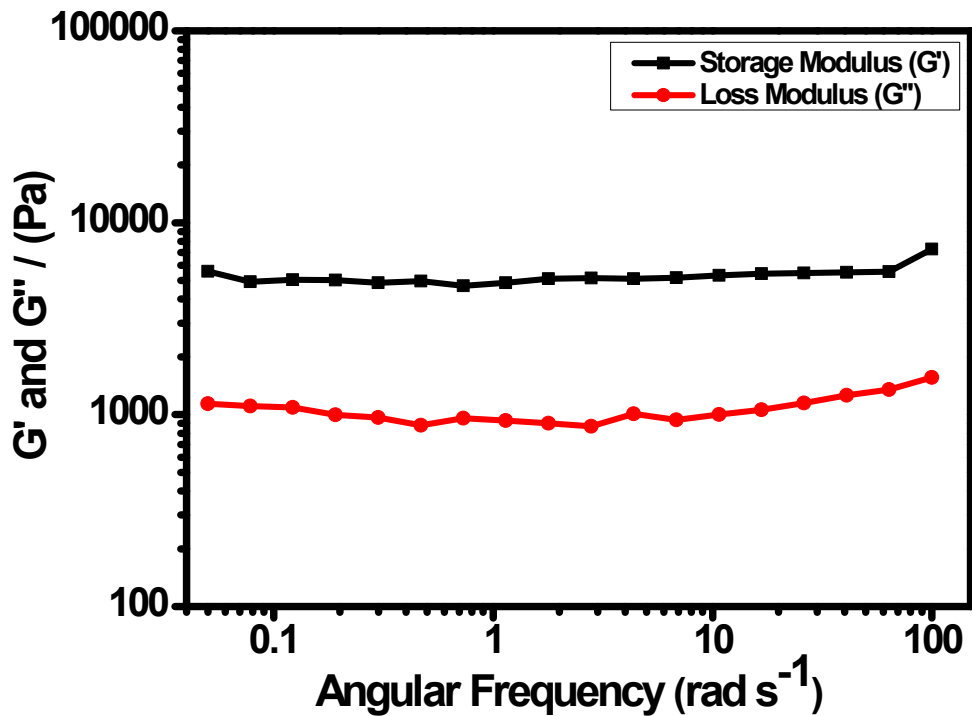


Fig. S21(b) The dynamic frequency sweep rheometry of CuG1. (Storage modulus G' is higher than the loss modulus G'').

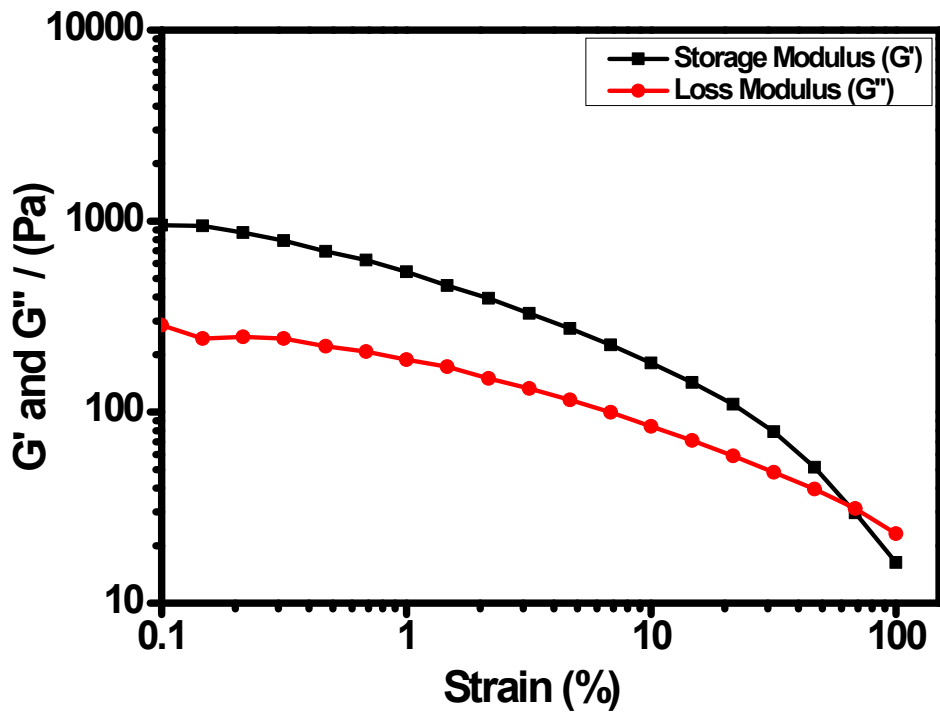


Fig. S22(a) Linear viscoelastic (LVE) property of **ZnG1**.

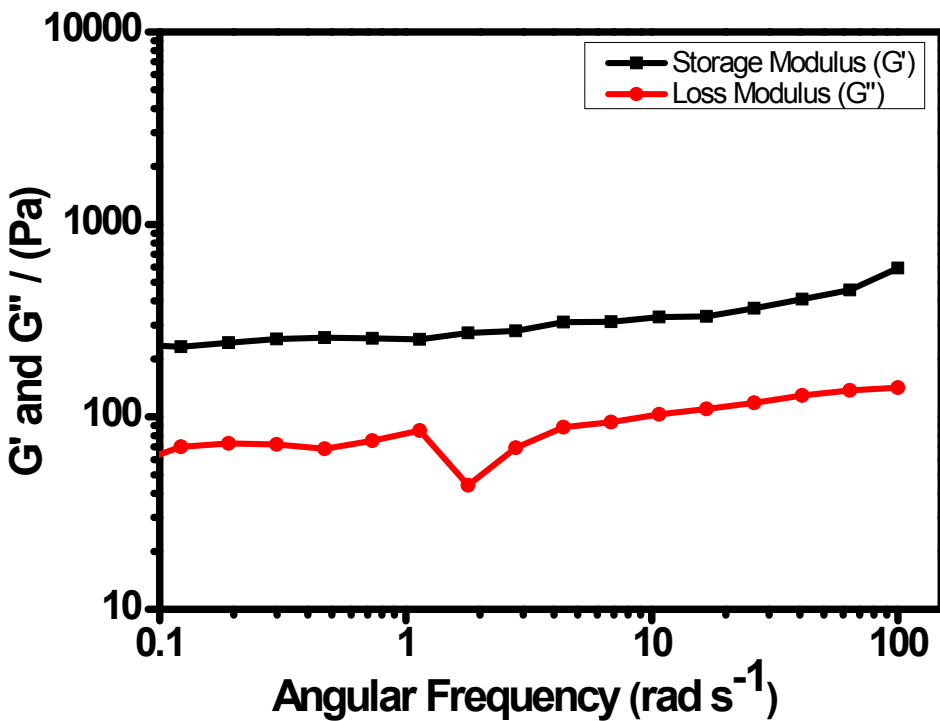


Fig. S22(b) The dynamic frequency sweep rheometry of **ZnG1**. (Storage modulus G' is higher than the loss modulus G'').

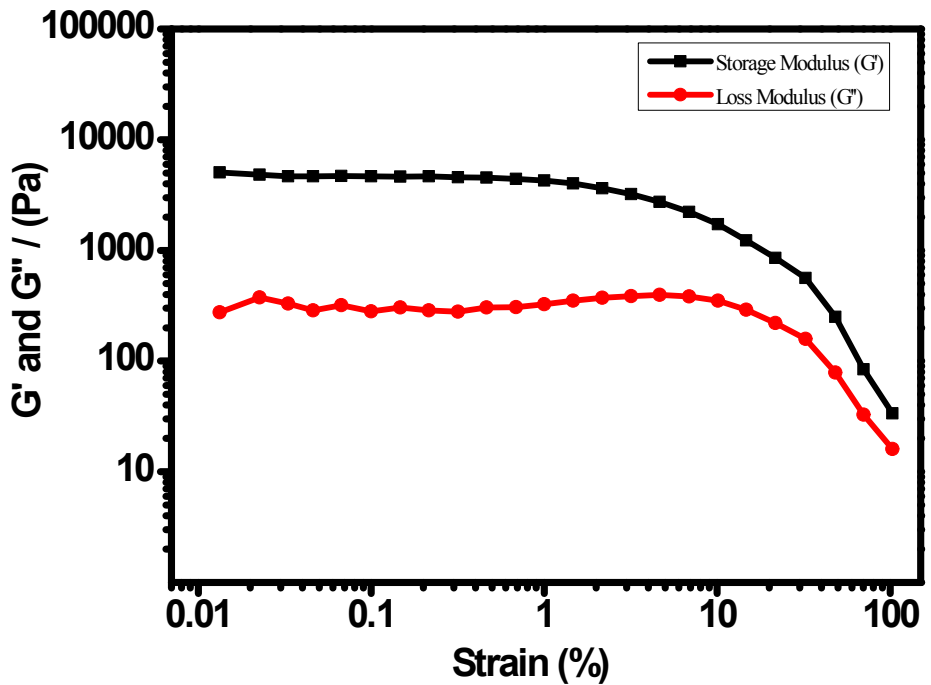


Fig. S23(a) Linear viscoelastic (LVE) property of NiG1.

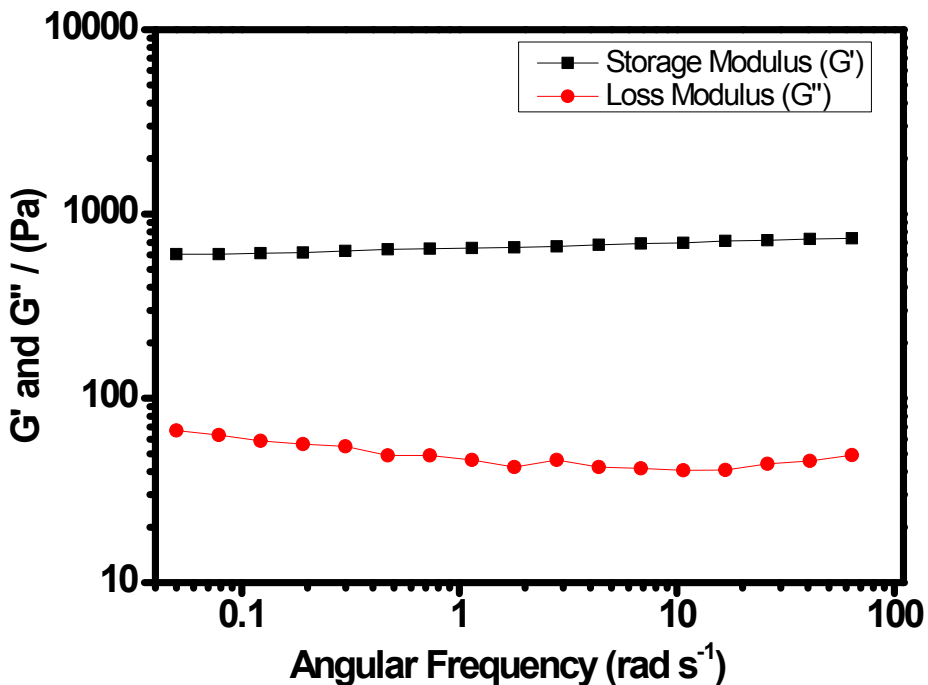


Fig. S23(b) The dynamic frequency sweep rheometry of NiG1. (Storage modulus G' is higher than the loss modulus G'').

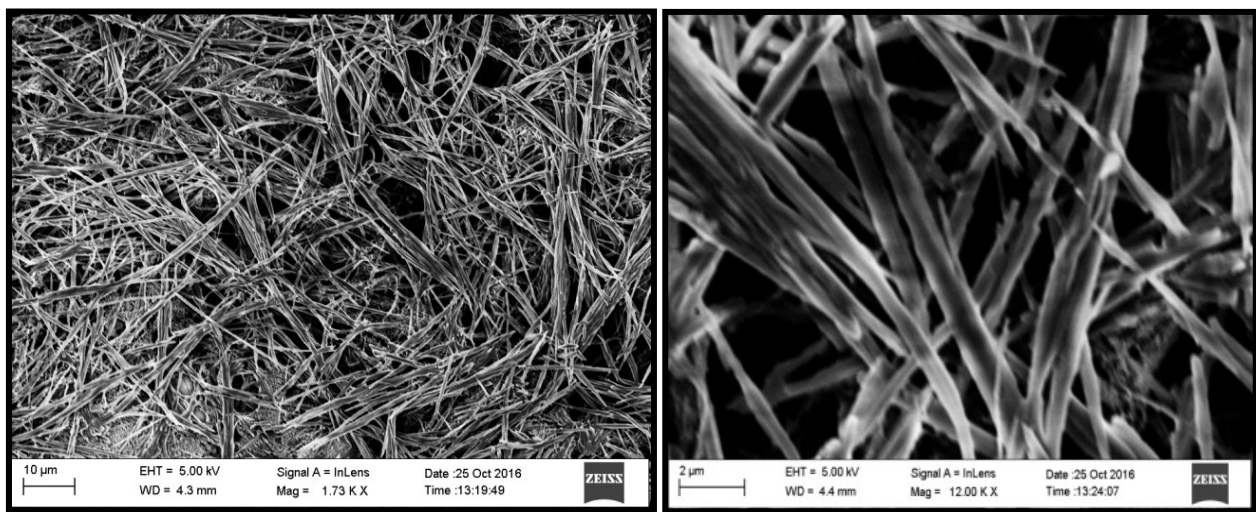


Fig. S24 SEM images of xerogel of ZnG1.

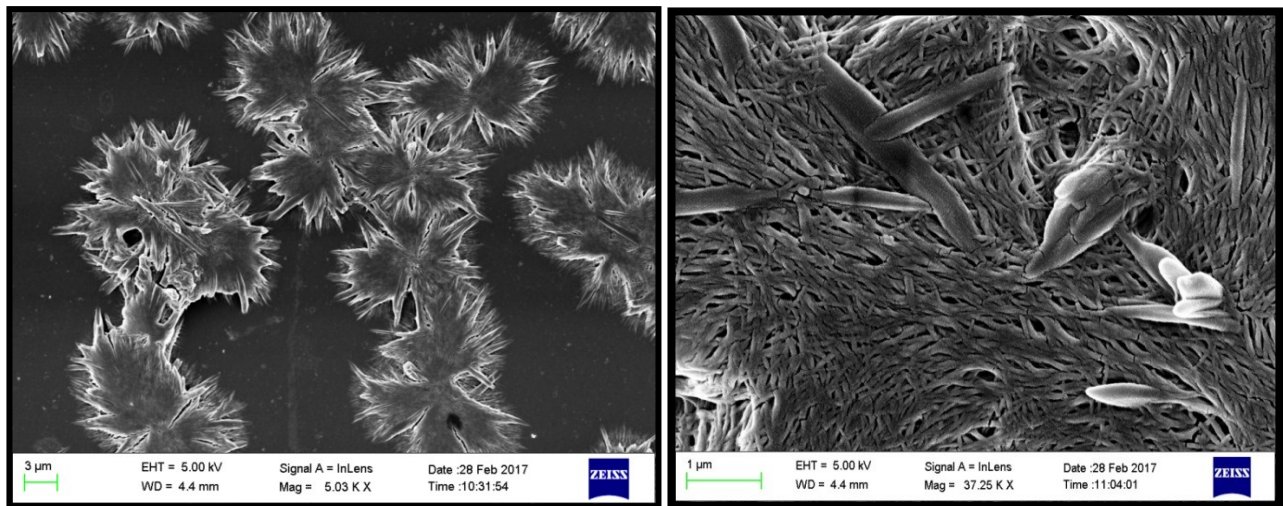


Fig. S25 SEM images of xerogel of NiG1.

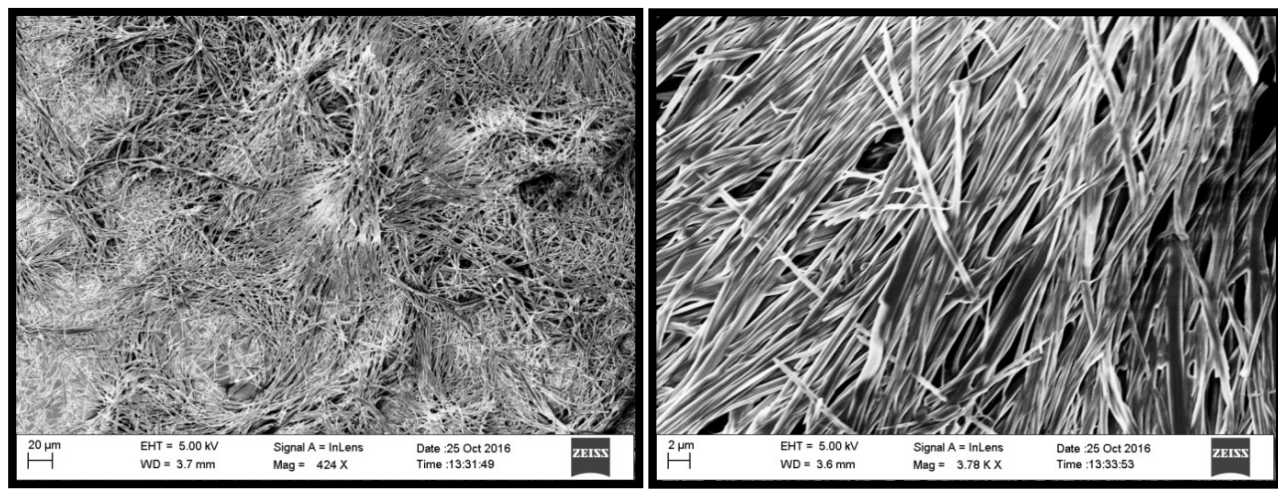


Fig. S26 SEM images of xerogel of **FeG1**.

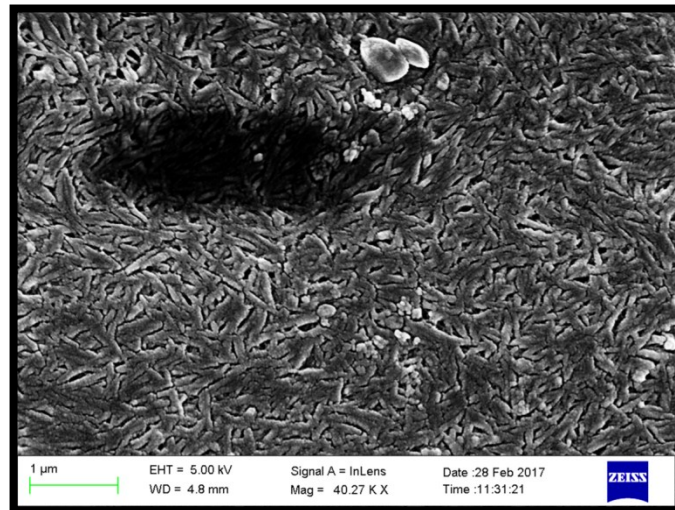


Fig. S27 SEM images of xerogel of **CuG1**.

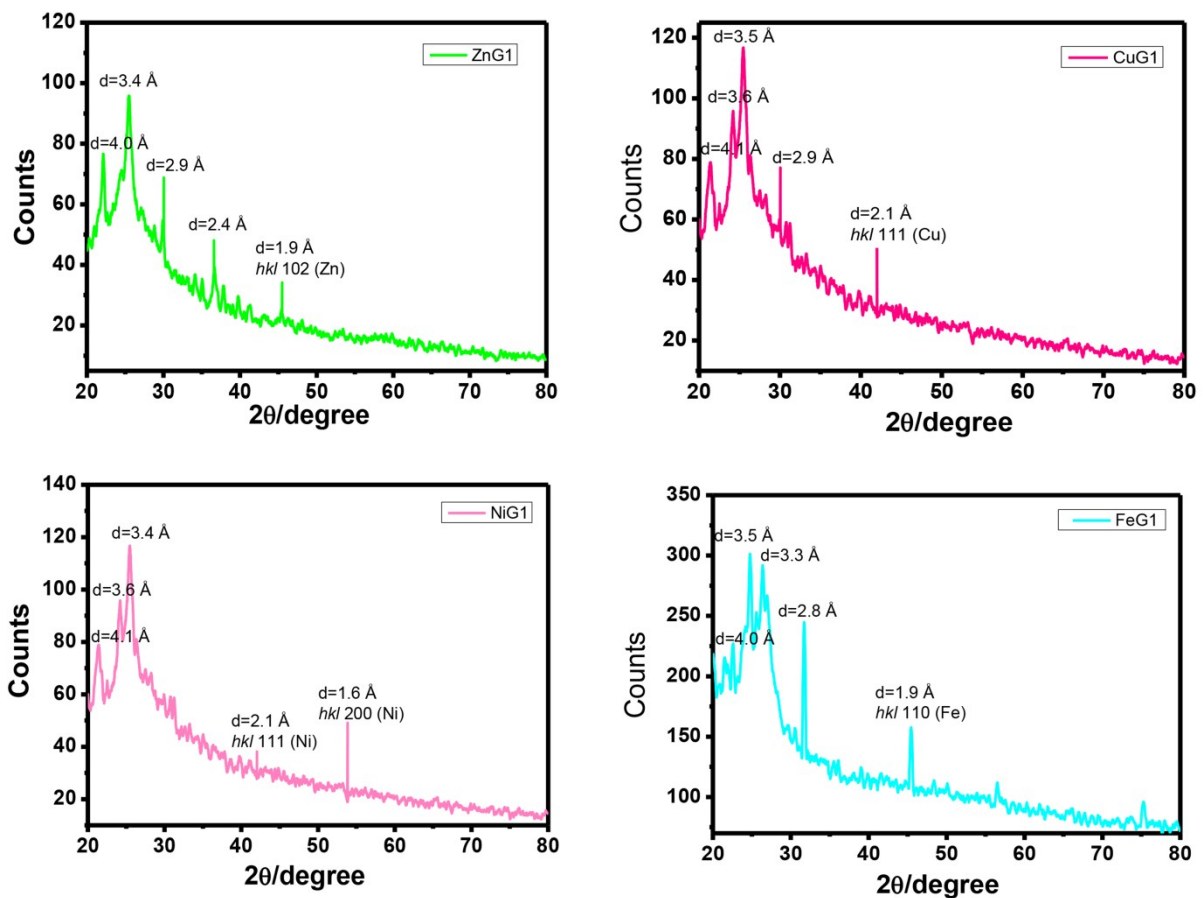


Fig. S28 Powder XRD patterns of xerogel of **FeG1**, **CuG1**, **ZnG1**, **NiG1**.

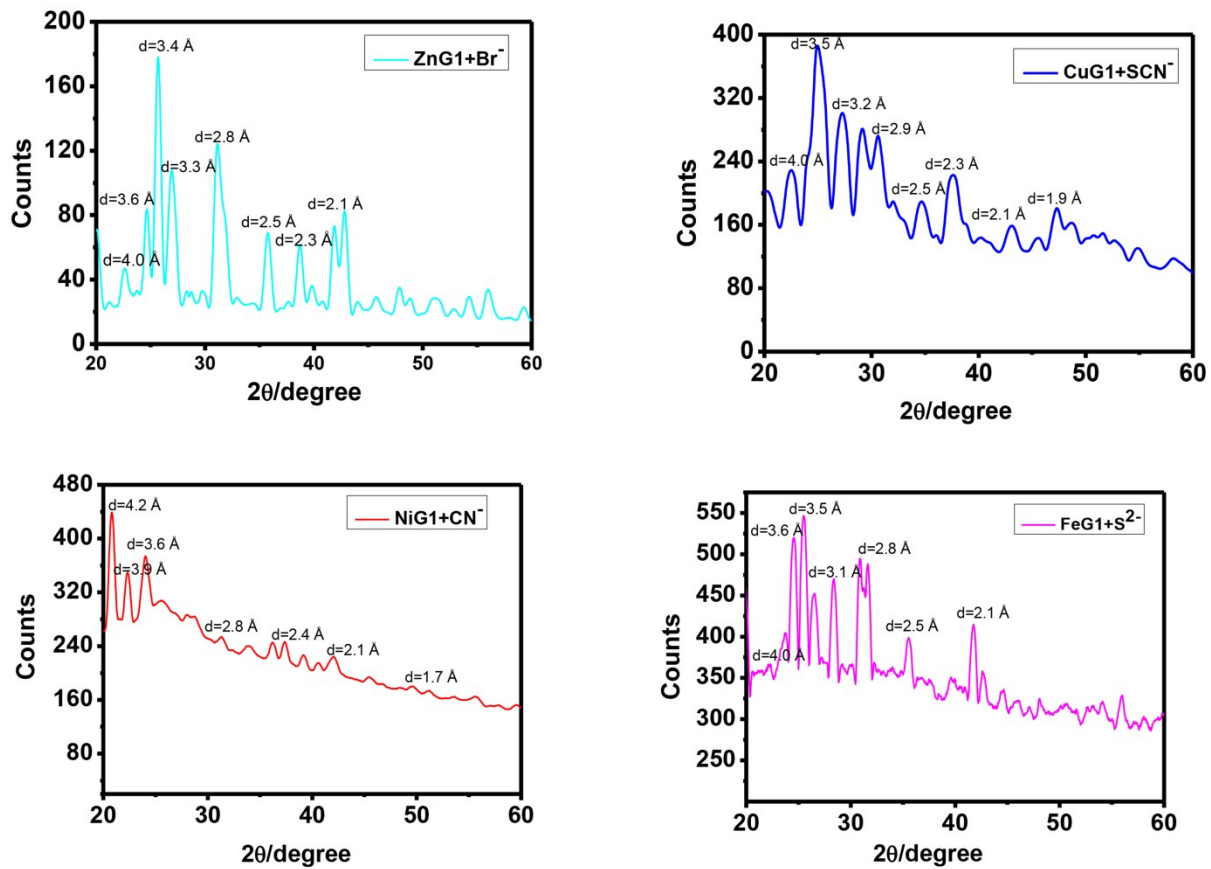


Fig. S29. Powder XRD patterns of xerogel of **ZnG1+Br⁻**, **CuG1+SCN⁻**, **NiG1+CN⁻**, **FeG1+S²⁻**.